Universität Hamburg
DER FORSCHUNG | DER LEHRE | DER BILDUNG

CLUSTER OF EXCELLENCE
QUANTUM UNIVERSE

DESY.

Juhi Dutta, Jayita Lahiri, Cheng Li, Gudrid Moortgat-Pick, Sheikh Farah Tabira, •Julia Ziegler

Benchmarking Dark Matter Candidates in 2HDMS: Prospects for Fututre Colliders

arXiv: 2504.14529

$$V_{SM} = -\mu^2 \Phi^\dagger \Phi + \lambda (\Phi^\dagger \Phi)^2$$

[Credit: Kateryna Radchenko]

arXiv: 2504.14529

$$V_{SM} = -\mu^2 \Phi^\dagger \Phi + \lambda(\Phi^\dagger \Phi)^2$$

?

Explain:

- cold dark matter (DM)

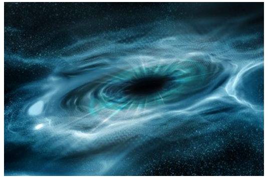

- 95 GeV excess (at LHC and LEP)

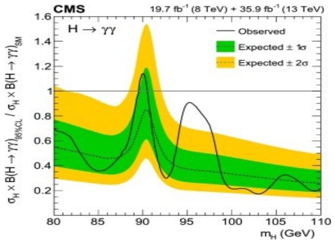

[Credit: Kateryna Radchenko]

arXiv: 2504.14529

$$V_{SM} = -\mu^2 \Phi^\dagger \Phi + \lambda(\Phi^\dagger \Phi)^2$$

?

- Dark Matter (DM)
- 95 GeV Excess

$$V_{2HDMS} = V_{2HDM} + V_S$$

[Credit: Kateryna Radchenko]

arXiv: 2504.14529

$$V_{SM} = -\mu^2 \Phi^\dagger \Phi + \lambda (\Phi^\dagger \Phi)^2$$

?

- Dark Matter (DM)
- 95 GeV Excess

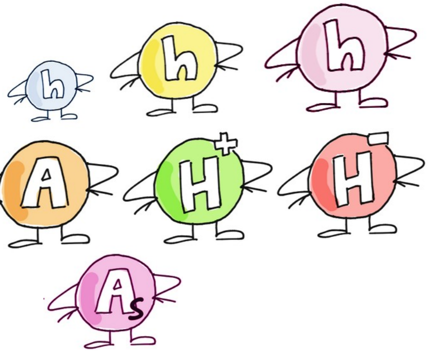

$$V_{2HDMS} = V_{2HDM} + V_S$$

Dark Matter (DM) Phenomenology
(Relic Density, Indirect Detection, Direct Detection)

SARAH
SPheno
micrOMEGAs

Collider Phenomenology
(HL-LHC, Future Lepton Colliders)

Pythia
Delphes
MadAnalysis
WHIZARD
Madgraph

[Credit: Kateryna Radchenko]

2HDMS Type II, Higgs Sector Potential

[Notation as in: Baum and Shah, arXiv: 1808.02667]

$$V = V_{2HDM} + V_S$$

$$V_{2HDM} = m_{11}^2 \Phi_1^\dagger \Phi_1 + m_{22}^2 \Phi_2^\dagger \Phi_2 - [m_{12}^2 \Phi_1^\dagger \Phi_2 + h.c.] + \frac{\lambda_1}{2}(\Phi_1^\dagger \Phi_1)^2 + \frac{\lambda_2}{2}(\Phi_2^\dagger \Phi_2)^2 + \lambda_3 (\Phi_1^\dagger \Phi_1)(\Phi_2^\dagger \Phi_2) + \lambda_4 (\Phi_1^\dagger \Phi_2)(\Phi_2^\dagger \Phi_1) + \left[\frac{\lambda_5}{2}(\Phi_1^\dagger \Phi_2)^2 + h.c.\right]$$

$$V_S = m_S^2 S^\dagger S + \left[\frac{m_S'^2}{2} S^2 + h.c.\right] + \left[\frac{\lambda_1''}{24} S^4 + h.c.\right] + \left[\frac{\lambda_2''}{6}(S^2 S^\dagger S) + h.c.\right] + \frac{\lambda_3''}{4}(S^\dagger S)^2 + S^\dagger S[\lambda_1' \Phi_1^\dagger \Phi_1 + \lambda_2' \Phi_2^\dagger \Phi_2] + [S^2(\lambda_4' \Phi_1^\dagger \Phi_1 + \lambda_5' \Phi_2^\dagger \Phi_2) + h.c.]$$

for this study:
$\lambda_2'' = \lambda_1''$

Type II, Couplings to Fermions

Down-type quarks	Leptons	Up-type quarks
Φ_1	Φ_1	Φ_2

V_{2HDMS} Symmetries

$\Phi_j \xrightarrow{U(1)} e^{i\theta}\Phi_j$ $\Phi_j^\dagger \xrightarrow{U(1)} e^{-i\theta}\Phi_j^\dagger$	avoids charge-parity violation
$\Phi_1 \xrightarrow{Z_2} -\Phi_1$ $\Phi_2 \xrightarrow{Z_2} \Phi_2$ (softly broken by m_{12}^2)	avoids flavour changing neutral currents
$\Phi_j \xrightarrow{Z_2'} \Phi_j$ $S \xrightarrow{Z_2'} -S$	stabilization of DM

2HDMS Type II, Higgs Sector Potential

[Notation as in: Baum and Shah, arXiv: 1808.02667]

$$V = V_{2HDM} + V_S$$

$$\begin{aligned}
V_{2HDM} = {} & m_{11}^2 \Phi_1^\dagger \Phi_1 + m_{22}^2 \Phi_2^\dagger \Phi_2 - [m_{12}^2 \Phi_1^\dagger \Phi_2 + h.c.] + \frac{\lambda_1}{2}(\Phi_1^\dagger \Phi_1)^2 \\
& + \frac{\lambda_2}{2}(\Phi_2^\dagger \Phi_2)^2 + \lambda_3 (\Phi_1^\dagger \Phi_1)(\Phi_2^\dagger \Phi_2) + \lambda_4 (\Phi_1^\dagger \Phi_2)(\Phi_2^\dagger \Phi_1) \\
& + \left[\frac{\lambda_5}{2} (\Phi_1^\dagger \Phi_2)^2 + h.c. \right]
\end{aligned}$$

$$\begin{aligned}
V_S = {} & m_S^2 S^\dagger S + \left[\frac{m_S'^2}{2} S^2 + h.c. \right] \\
& + \left[\frac{\lambda_1''}{24} S^4 + h.c. \right] + \left[\frac{\lambda_2''}{6} (S^2 S^\dagger S) + h.c. \right] + \frac{\lambda_3''}{4} (S^\dagger S)^2 \\
& + S^\dagger S [\lambda_1' \Phi_1^\dagger \Phi_1 + \lambda_2' \Phi_2^\dagger \Phi_2] + [S^2 (\lambda_4' \Phi_1^\dagger \Phi_1 + \lambda_5' \Phi_2^\dagger \Phi_2) + h.c.]
\end{aligned}$$

for this study:
$\lambda_2'' = \lambda_1''$

$$\Phi_i = \begin{pmatrix} \phi_i^+ \\ \frac{1}{\sqrt{2}}(v_i + \rho_i + i\eta_i) \end{pmatrix} \qquad \langle \Phi_i \rangle = \begin{pmatrix} 0 \\ \frac{v_i}{\sqrt{2}} \end{pmatrix}$$

$$S = \frac{1}{\sqrt{2}}(v_S + \rho_S + iA_S) \qquad \langle S \rangle = \frac{v_S}{\sqrt{2}}$$

DM Candidate

DM Properties:

- massive
- electrically neutral
- colourless
- stable

DM mass:

$$m_{A_S}^2 = \frac{\partial^2 V}{\partial A_S^\dagger \partial A_S} \Big|_{\Phi_1 = \langle \Phi_1 \rangle \;\; \Phi_2 = \langle \Phi_2 \rangle, \;\; S = \langle S \rangle}$$

$$= -(2 m_S'^2 + v_S^2 (\frac{\lambda_1''}{3} + \frac{\lambda_1''}{3}) + 2(\lambda_4' v_1^2 + \lambda_5' v_2^2))$$

2HDMS Type II, Higgs Sector Potential

[Notation as in: Baum and Shah, arXiv: 1808.02667]

$$V = V_{2HDM} + V_S$$

$$\begin{aligned}
V_{2HDM} = {} & m_{11}^2 \Phi_1^\dagger \Phi_1 + m_{22}^2 \Phi_2^\dagger \Phi_2 - [m_{12}^2 \Phi_1^\dagger \Phi_2 + h.c.] + \frac{\lambda_1}{2}(\Phi_1^\dagger \Phi_1)^2 \\
& + \frac{\lambda_2}{2}(\Phi_2^\dagger \Phi_2)^2 + \lambda_3 (\Phi_1^\dagger \Phi_1)(\Phi_2^\dagger \Phi_2) + \lambda_4 (\Phi_1^\dagger \Phi_2)(\Phi_2^\dagger \Phi_1) \\
& + \left[\frac{\lambda_5}{2}(\Phi_1^\dagger \Phi_2)^2 + h.c.\right]
\end{aligned}$$

$$\begin{aligned}
V_S = {} & m_S^2 S^\dagger S + \left[\frac{m_S'^2}{2} S^2 + h.c.\right] \\
& + \left[\frac{\lambda_1''}{24} S^4 + h.c.\right] + \left[\frac{\lambda_2''}{6}(S^2 S^\dagger S) + h.c.\right] + \frac{\lambda_3''}{4}(S^\dagger S)^2 \\
& + S^\dagger S[\lambda_1' \Phi_1^\dagger \Phi_1 + \lambda_2' \Phi_2^\dagger \Phi_2] + [S^2(\lambda_4' \Phi_1^\dagger \Phi_1 + \lambda_5' \Phi_2^\dagger \Phi_2) + h.c.]
\end{aligned}$$

for this study:
$\lambda_2'' = \lambda_1''$

Higgs Sector particles:

2 charged: $H_\pm$,

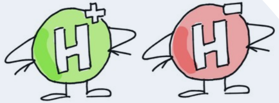

1 charged GB: $G_\pm$,

3 scalars: h_1, h_2, h_3,

SM-like

1 pseudo scalar: A,

1 pseudo scalar GB: G_0,

1 DM: A_S

$$\begin{pmatrix} h_1 \\ h_2 \\ h_3 \end{pmatrix} = R(\alpha_{1,2,3}) \begin{pmatrix} \rho_1 \\ \rho_2 \\ \rho_3 \end{pmatrix}$$

$$v = \sqrt{v_1^2 + v_2^2}$$

$$\tan(\beta) = \frac{v_2}{v_1}$$

2HDMS Type II, Higgs Sector Potential

[Notation as in: Baum and Shah, arXiv: 1808.02667]

$$V = V_{2HDM} + V_S$$

$$\begin{aligned} V_{2HDM} = {} & m_{11}^2 \Phi_1^\dagger \Phi_1 + m_{22}^2 \Phi_2^\dagger \Phi_2 - [m_{12}^2 \Phi_1^\dagger \Phi_2 + h.c.] + \frac{\lambda_1}{2} (\Phi_1^\dagger \Phi_1)^2 \\ & + \frac{\lambda_2}{2} (\Phi_2^\dagger \Phi_2)^2 + \lambda_3 (\Phi_1^\dagger \Phi_1)(\Phi_2^\dagger \Phi_2) + \lambda_4 (\Phi_1^\dagger \Phi_2)(\Phi_2^\dagger \Phi_1) \\ & + \left[\frac{\lambda_5}{2} (\Phi_1^\dagger \Phi_2)^2 + h.c. \right] \end{aligned}$$

$$\begin{aligned} V_S = {} & m_S^2 S^\dagger S + \left[\frac{m_S'^2}{2} S^2 + h.c. \right] \\ & + \left[\frac{\lambda_1''}{24} S^4 + h.c. \right] + \left[\frac{\lambda_2''}{6} (S^2 S^\dagger S) + h.c. \right] + \frac{\lambda_3''}{4} (S^\dagger S)^2 \\ & + S^\dagger S [\lambda_1' \Phi_1^\dagger \Phi_1 + \lambda_2' \Phi_2^\dagger \Phi_2] + [S^2 (\lambda_4' \Phi_1^\dagger \Phi_1 + \lambda_5' \Phi_2^\dagger \Phi_2) + h.c.] \end{aligned}$$

for this study:
$\lambda_2''=\lambda_1''$

DM Portal Couplings:

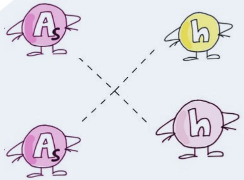

$$\lambda_{h_j h_k A_S A_S} = \frac{\partial^4 V}{\partial h_j \partial h_k \partial A_S \partial A_S}$$

$$= -i[(\lambda_1' - 2\lambda_4') R_{j1} R_{k1} + (\lambda_2' - 2\lambda_5') R_{j2} R_{k2} - \frac{1}{2} (\lambda_1'' - \lambda_3'') R_{j3} R_{k3}]$$

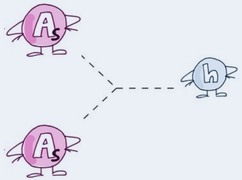

$$\frac{\lambda_{h_j A_S A_S}}{v} = \frac{1}{v} \frac{\partial^3 V}{\partial h_j \partial A_S \partial A_S}$$

$$= -i[(\lambda_1' - 2\lambda_4') c_\beta R_{j1} + (\lambda_2' - 2\lambda_5') s_\beta R_{j2} - \frac{v_S}{2v} (\lambda_1'' - \lambda_3'') R_{j3}]$$

arXiv: 2504.14529

$$V_{SM} = -\mu^2 \Phi^\dagger \Phi + \lambda (\Phi^\dagger \Phi)^2$$

?

- Dark Matter (DM)
- 95 GeV Excess

$$V_{2HDMS} = V_{2HDM} + V_S$$

Dark Matter (DM) Phenomenology

(Relic Density, Indirect Detection, Direct Detection)

SARAH
SPheno
micrOMEGAs

Collider Phenomenology

(HL-LHC, Future Lepton Colliders)

Pythia
Delphes
MadAnalysis
WHIZARD
Madgraph

[Credit: Kateryna Radchenko]

arXiv: 2504.14529

$$V_{SM} = -\mu^2 \Phi^\dagger \Phi + \lambda (\Phi^\dagger \Phi)^2$$

?
- Dark Matter (DM)
- 95 GeV Excess

- Type II
- U(1), Z_2, Z_2'
- DM candidate A_s

$$V_{2HDMS} = V_{2HDM} + V_S$$

Dark Matter (DM) Phenomenology

(Relic Density, Indirect Detection, Direct Detection)

SARAH
SPheno
micrOMEGAs

Collider Phenomenology

(HL-LHC, Future Lepton Colliders)

Pythia
Delphes
MadAnalysis
WHIZARD
Madgraph

[Credit: Kateryna Radchenko]

arXiv: 2504.14529

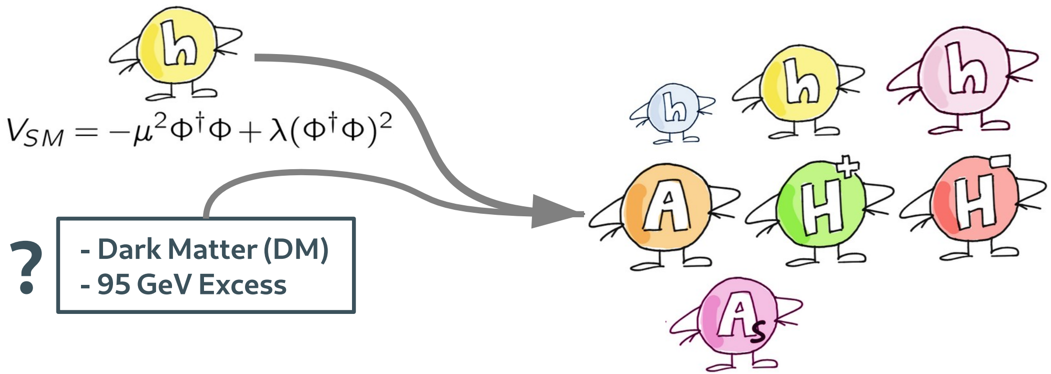

- Type II
- U(1), Z_2, Z_2'
- DM candidate A_s

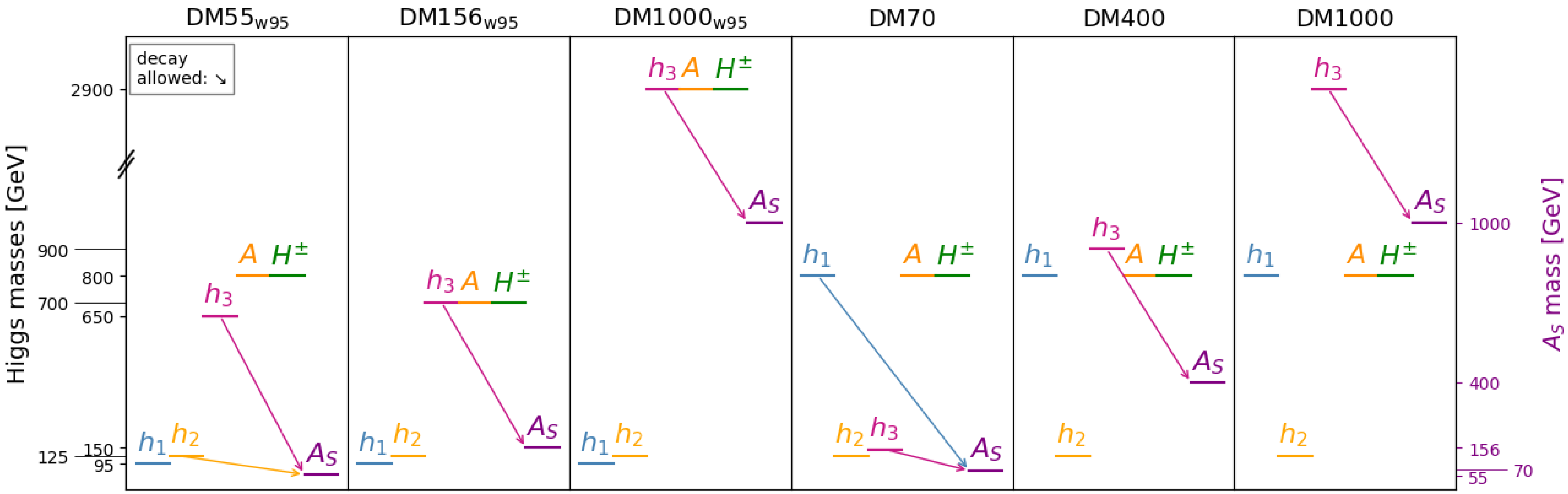

arXiv: 2504.14529

$V_{SM} = -\mu^2\Phi^\dagger\Phi + \lambda(\Phi^\dagger\Phi)^2$

?
- Dark Matter (DM)
- 95 GeV Excess

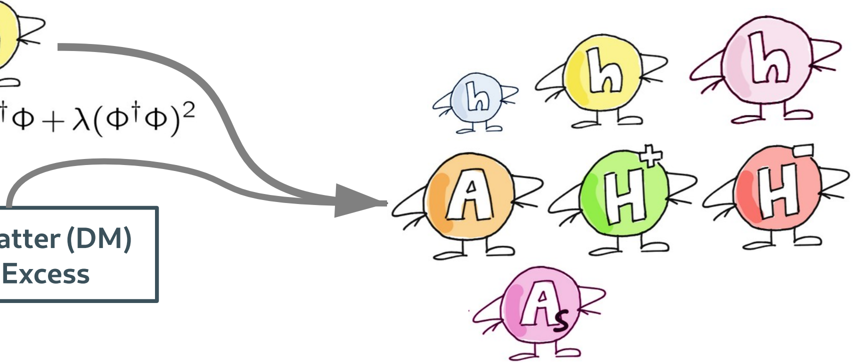

- Type II
- U(1), Z_2, Z_2'
- DM candidate A_s

Constraints:
- Theoretical: bfb, unitarity
- Experimental: HiggsBounds, Planck, LUX-ZEPLIN, Fermi-LAT

*including 95 GeV excess

*γγ channel at CMS (~2.9 σ), bb channel at LEP (~2 σ), investigated in S. Heinemeyer, C. Li, et al, 2021, arxiv:2112.11958

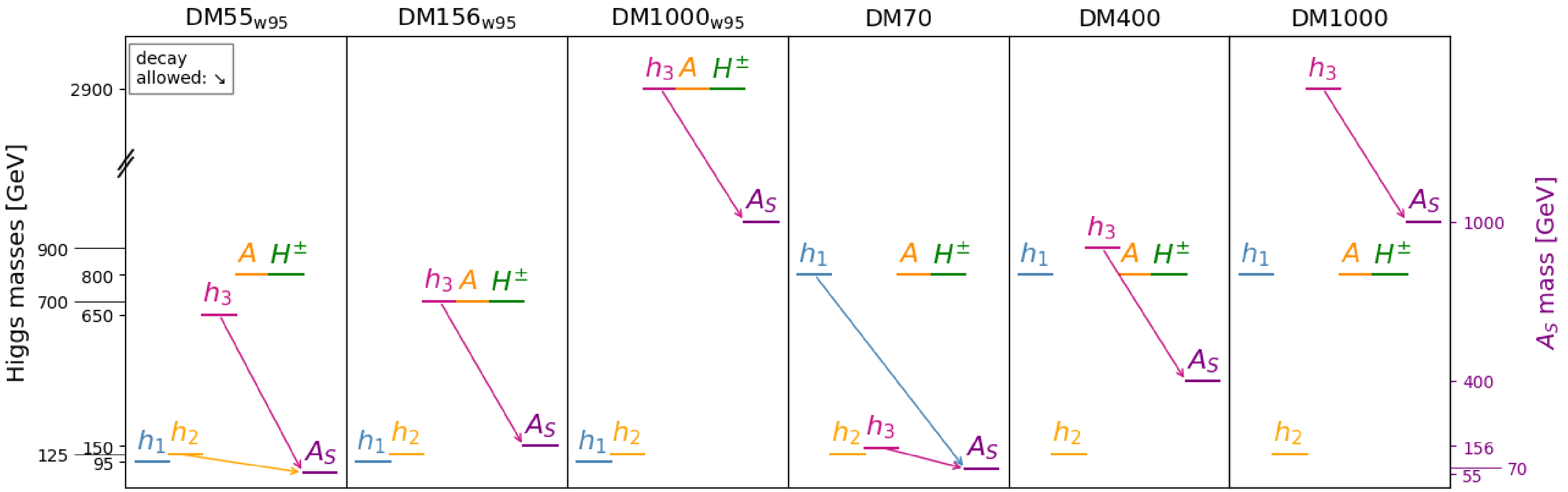

arXiv: 2504.14529

$V_{SM} = -\mu^2\Phi^\dagger\Phi + \lambda(\Phi^\dagger\Phi)^2$

?

- Dark Matter (DM)
- 95 GeV Excess

$V_{2HDMS} = V_{2HDM} + V_S$

- Type II
- U(1), Z_2, Z_2'
- DM candidate A_s

Constraints:
- Theoretical: bfb, unitarity
- Experimental: HiggsBounds, Planck, LUX-ZEPLIN, Fermi-LAT
*including 95 GeV excess

*$\gamma\gamma$ channel at CMS (~2.9 σ), bb channel at LEP (~2 σ), investigated in S. Heinemeyer, C. Li, et al, 2021, arxiv:2112.11958

Dark Matter (DM) Phenomenology

(Relic Density, Indirect Detection, Direct Detection)

SARAH
SPheno
micrOMEGAs

Collider Phenomenology

(HL-LHC, Future Lepton Colliders)

Pythia
Delphes
MadAnalysis
WHIZARD
Madgraph

[Credit: Kateryna Radchenko]

DM Phenomenology

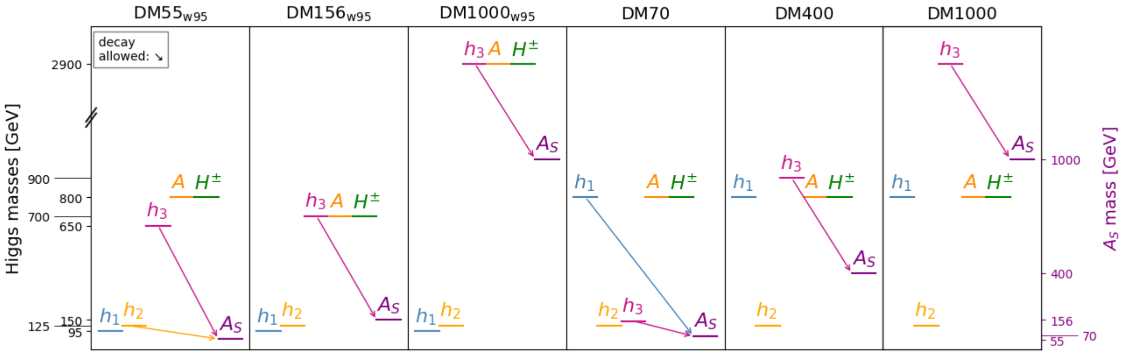

Relic Density

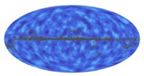

(=amount of DM left in universe today),
constraints from Planck : $\Omega h^2 \approx 0.12$

Direct Detection CS

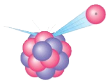

(=elastic scattering of DM on nucleon),
constraints from LUX-ZEPLIN (LZ)

Indirect Detection CS

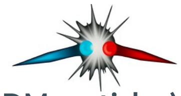

(=annihilation of two DM particles),
constraints from Fermi-LAT

Benchmark	Ωh^2	σ_{pA_S}/pb	σ_{nA_S}/pb	$\sigma_{A_S A_S \to XX}/\frac{cm^3}{s}$	$BR(h_3 \to A_S A_S)$	$BR(h_2 \to A_S A_S)$	$BR(h_1 \to A_S A_S)$
$DM55_{w95}$	0.11	4.21×10^{-12}	4.08×10^{-12}	1.98×10^{-28}	3.81×10^{-9}	0.0199	-
$DM156_{w95}$	1.61×10^{-4}	3.903×10^{-11}	4.160×10^{-11}	3.875×10^{-29}	0.69	-	-
$DM1000_{w95}$	0.111	3.323×10^{-11}	3.369×10^{-11}	2.045×10^{-26}	0.0359	-	-
DM70	0.113	8.938×10^{-16}	2.651×10^{-13}	2.13×10^{-28}	0.99934	-	1.80×10^{-4}
DM400	0.106	4.960×10^{-11}	5.101×10^{-11}	3.67×10^{-26}	0.82203	-	-
DM1000	0.117	8.263×10^{-11}	8.464×10^{-11}	2.018×10^{-26}	0.005	-	-

Collider Phenomenology

Hadron Collider
(HL-LHC)

e+e- Colliders
(ILC, FCC-ee, CEPC, CLIC)

μ+μ- Collider

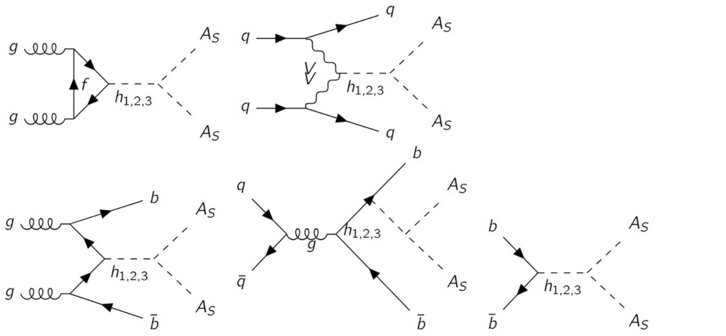

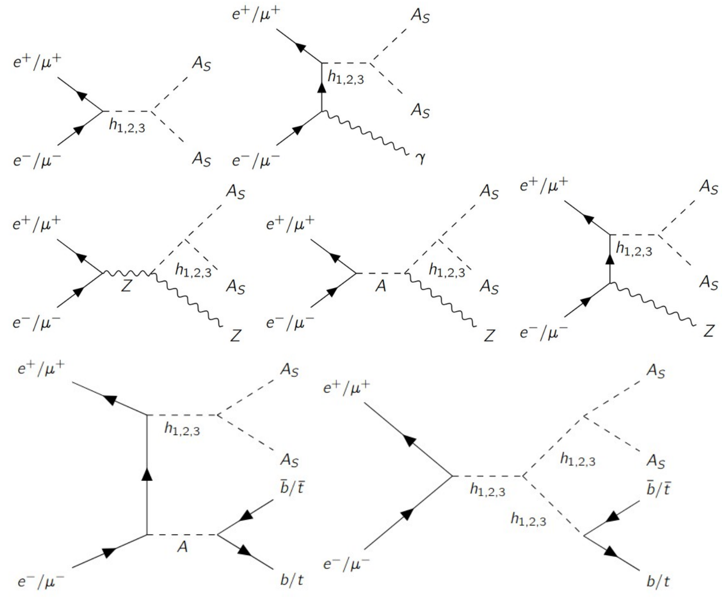

Collider Phenomenology, HL-LHC

Process	Production cross-section (fb) at $\sqrt{s} = 14$ TeV		
	DM55$_{\text{w95}}$	**DM156$_{\text{w95}}$**	**DM70**
GGF($h_2 \to A_S A_S$)	★ 533.9	-	★ 19.29×10^3
GGF($h_3 \to A_S A_S$)	-	0.015	-
VBF($h_2 \to A_S A_S$)	54.33	-	★ 2.72×10^3
VBF($h_3 \to A_S A_S$)	-	0.134	0.0022
BBH (($b\bar{b}h_2 \to A_S A_S$))	21.6	-	0.137
BBH (($b\bar{b}h_3 \to A_S A_S$))	-	★ 47.24	-

Process	Production cross-section (fb) at $\sqrt{s} = 14$ TeV		
	DM400	**DM1000**	**DM1000$_{\text{w95}}$**
GGF($h_3 \to A_S A_S$)	0.013	6.35×10^{-7}	4.5×10^{-6}
VBF($h_3 \to A_S A_S$)	0.0008	-	-
BBH($h_3 \to A_S A_S$)	0.007	-	-

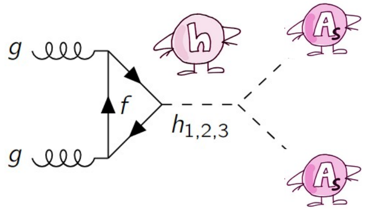

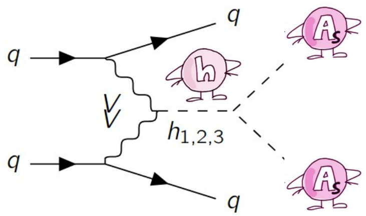

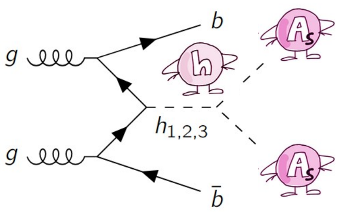

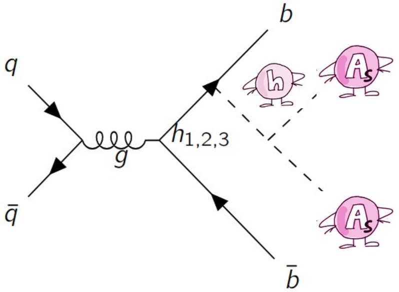

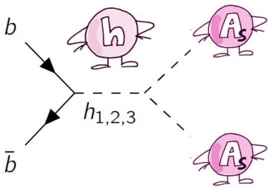

Collider Phenomenology, HL-LHC

Process	Production cross-section (fb) at $\sqrt{s} = 14$ TeV		
	DM55$_{\mathbf{w95}}$	**DM156$_{\mathbf{w95}}$**	**DM70**
GGF($h_2 \to A_S A_S$)	★ 533.9	-	★ 19.29×10^3
GGF($h_3 \to A_S A_S$)	-	0.015	-
VBF($h_2 \to A_S A_S$)	54.33	-	★ 2.72×10^3
VBF($h_3 \to A_S A_S$)	-	0.134	0.0022
BBH (($b\bar{b}h_2 \to A_S A_S$))	21.6	-	0.137
BBH (($b\bar{b}h_3 \to A_S A_S$))	-	★ 47.24	-

Process	Production cross-section (fb) at $\sqrt{s} = 14$ TeV		
	DM400	**DM1000**	**DM1000$_{\mathbf{w95}}$**
GGF($h_3 \to A_S A_S$)	0.013	6.35×10^{-7}	4.5×10^{-6}
VBF($h_3 \to A_S A_S$)	0.0008	-	-
BBH($h_3 \to A_S A_S$)	0.007	-	-

GGF

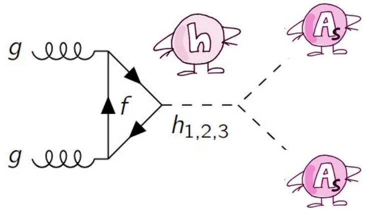

Benchmark	Significance
DM55$_{\mathbf{w95}}$	0.30σ
DM70	0.55σ

VBF

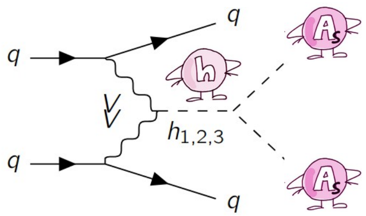

Benchmark	Significance
DM70	1.94σ

BBH

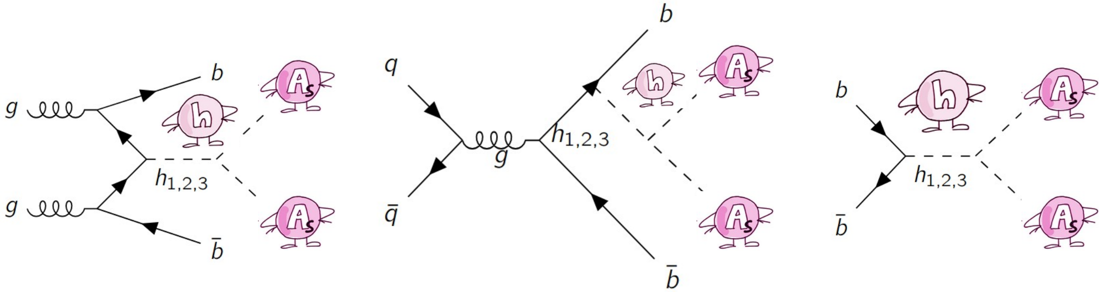

Benchmark	Significance
DM156$_{\mathbf{w95}}$	1.95σ

Collider Phenomenology, e^+e^- Colliders

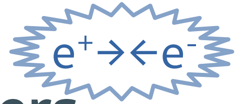

Z+MET

Benchmark	Production cross-section (fb)		
	at $\sqrt{s} = 250$ GeV	at $\sqrt{s} = 500$ GeV	at $\sqrt{s} = 1$ TeV
DM55$_{\mathbf{w95}}$	4.42	1.1	0.24
DM70	0.33	0.15	0.035
$\nu\bar{\nu}Z$ background	503	491	950

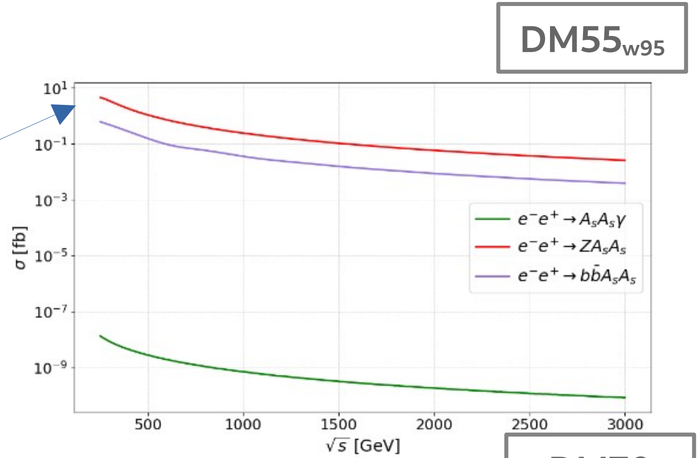

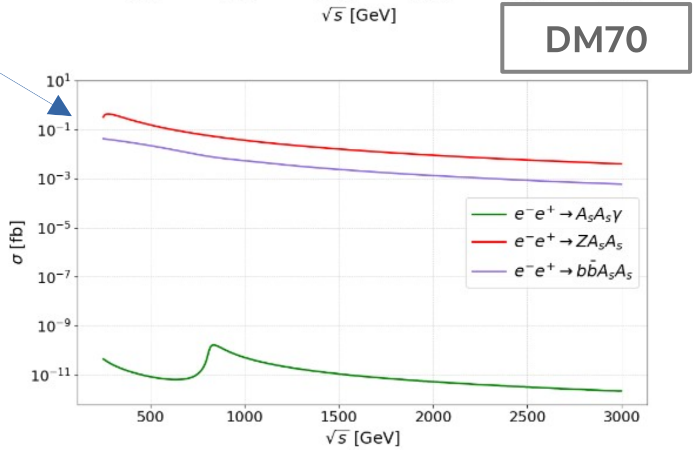

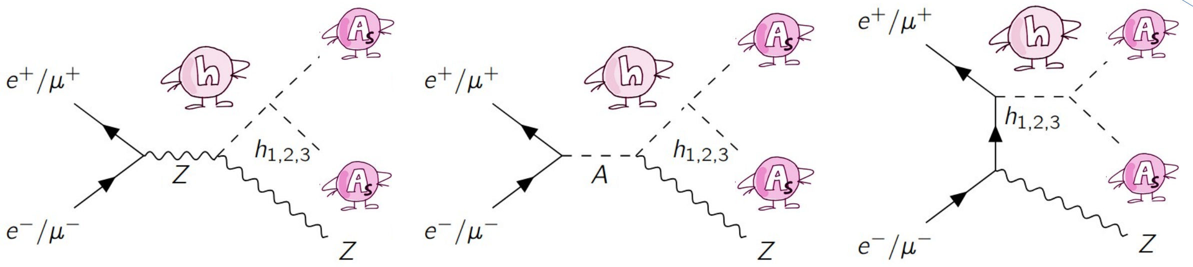

e⁺→←e⁻

Collider Phenomenology, e^+e^- Colliders

Z+MET

Benchmark	Production cross-section (fb)		
	at $\sqrt{s} = 250$ GeV	at $\sqrt{s} = 500$ GeV	at $\sqrt{s} = 1$ TeV
$\mathbf{DM55_{w95}}$	4.42	1.1	0.24
DM70	0.33	0.15	0.035
$\nu\bar{\nu}Z$ background	503	491	950

Benchmark	$\sqrt{s}$	Cut	Significance
$\mathbf{DM55_{w95}}$	250 GeV	$\not{M} > 100$ GeV	11σ ($1ab^{-1}$)
DM70	250 GeV	$\not{M} > 130$ GeV	3σ ($3ab^{-1}$)
$\mathbf{DM55_{w95}}$	500 GeV	$\not{M} > 100$ GeV and $\not{M} < 150$ GeV	3.6σ ($1ab^{-1}$)
DM70	500 GeV	$\not{M} > 140$ GeV and $\not{M} < 190$ GeV	1.5σ ($3ab^{-1}$)
$\mathbf{DM55_{w95}}$	1 TeV	$\not{M} > 120$ GeV and $\not{M} < 250$ GeV	2.4σ ($3ab^{-1}$)
DM70	1 TeV	$\not{M} > 120$ GeV and $\not{M} < 250$ GeV	0.36σ ($3ab^{-1}$)

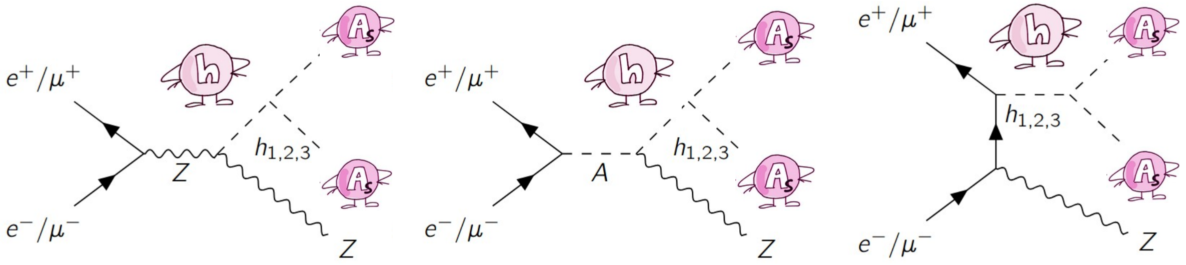

$\mu^+ \rightarrow \leftarrow \mu^-$

Collider Phenomenology, $\mu^+\mu^-$ Colliders

bb+MET

Benchmark	Production cross-section (fb)	
	at $\sqrt{s} = 3$ TeV	at $\sqrt{s} = 10$ TeV
DM156$_{w95}$	0.48	0.063
$b\bar{b}\nu\nu$ background	758	1.3
$t\bar{t}$ background	20	1.7

γ+MET

Benchmark	Production cross-section (fb)at $\sqrt{s} = 1$ TeV
DM156$_{w95}$	0.23
$\nu\nu\gamma$ background	2.45

tt+MET

Benchmark	Production cross-section (fb) at $\sqrt{s} = 10$ TeV
DM1000$_{w95}$	0.027
$t\bar{t}$+MET background	1.66

DM156$_{w95}$

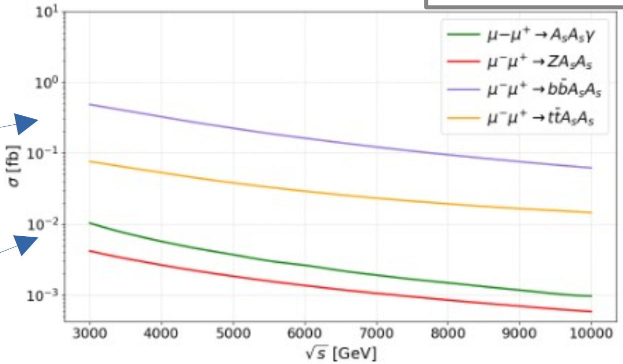

DM1000$_{w95}$

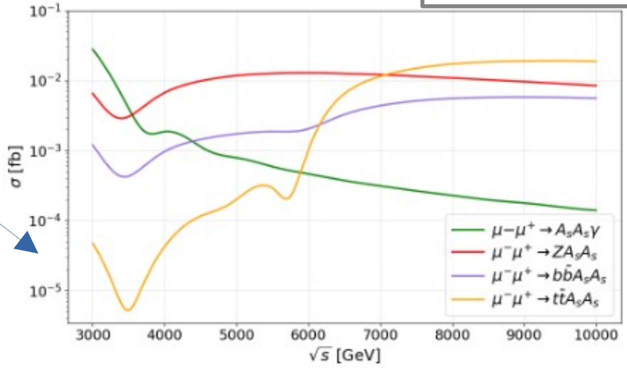

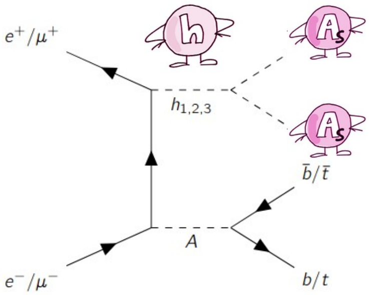

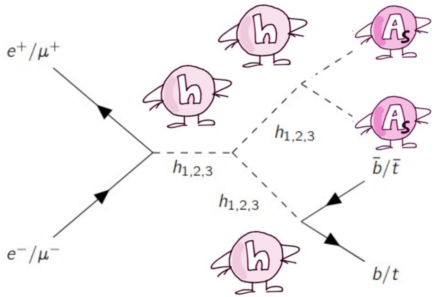

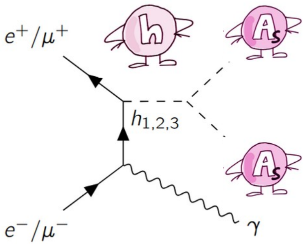

μ+→←μ-

Collider Phenomenology, $\mu^+\mu^-$ Colliders

bb+MET

Benchmark	Production cross-section (fb)	
	at $\sqrt{s} = 3$ TeV	at $\sqrt{s} = 10$ TeV
DM156$_{\mathbf{w95}}$	0.48	0.063
$b\bar{b}\nu\nu$ background	758	1.3
$t\bar{t}$ background	20	1.7

Benchmark	Cut	Significance
DM156$_{\mathbf{w95}}$	100 GeV $< m_{bb} <$ 500 GeV	6.3σ ($3ab^{-1}$)

γ+MET

Benchmark	Production cross-section (fb)at $\sqrt{s} = 1$ TeV
DM156$_{\mathbf{w95}}$	0.23
$\nu\nu\gamma$ background	2.45

Benchmark	Cut	Significance
DM156$_{\mathbf{w95}}$	690 GeV $< \not{M} <$ 710 GeV	3σ ($3ab^{-1}$), 5.3σ ($10ab^{-1}$)

tt+MET

Benchmark	Production cross-section (fb) at $\sqrt{s} = 10$ TeV
DM1000$_{\mathbf{w95}}$	0.027
$t\bar{t}$+MET background	1.66

Benchmark	Cut	Significance
DM1000$_{\mathbf{w95}}$	$m_{bb} <$ 2 TeV	2.9σ ($10ab^{-1}$)

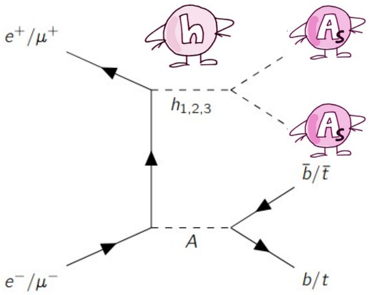

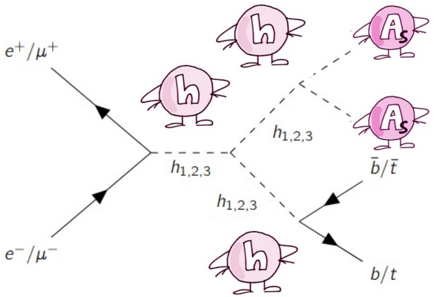

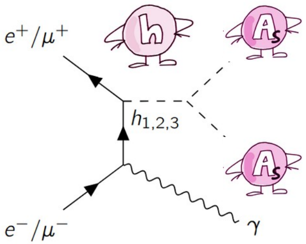

μ+→←μ-

Collider Phenomenology, $\mu^+\mu^-$ Colliders

bb+MET

Benchmark	Production cross-section (fb)	
	at $\sqrt{s} = 3$ TeV	at $\sqrt{s} = 10$ TeV
$\mathbf{DM156_{w95}}$	0.48	0.063
$b\bar{b}\nu\nu$ background	758	1.3
$t\bar{t}$ background	20	1.7

Benchmark	Cut	Significance
$\mathbf{DM156_{w95}}$	100 GeV $< m_{bb} <$ 500 GeV	6.3σ $(3ab^{-1})$

γ+MET

Benchmark	Production cross-section (fb)at $\sqrt{s} = 1$ TeV
$\mathbf{DM156_{w95}}$	0.23
$\nu\nu\gamma$ background	2.45

Benchmark	Cut	Significance
$\mathbf{DM156_{w95}}$	690 GeV $< \not{M} <$ 710 GeV	3σ $(3ab^{-1})$, 5.3σ $(10ab^{-1})$

tt+MET

Benchmark	Production cross-section (fb) at $\sqrt{s} = 10$ TeV
$\mathbf{DM1000_{w95}}$	0.027
$t\bar{t}$+MET background	1.66

Benchmark	Cut	Significance
$\mathbf{DM1000_{w95}}$	$m_{bb} <$ 2 TeV	2.9σ $(10ab^{-1})$

*results can be improved with polarized beams (higher signal rates, better background suppression)

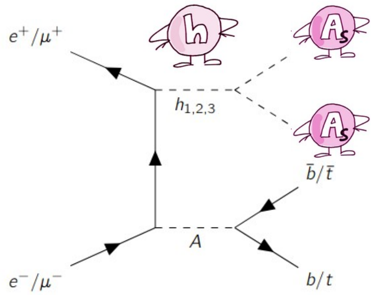

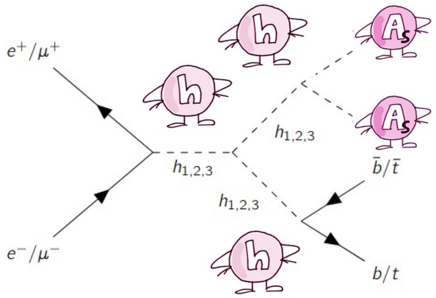

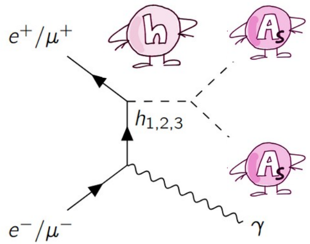

Collider Phenomenology, Challenging Scenarios

$\mu^+ \rightarrow \leftarrow \mu^-$

DM400

Final state	Production cross-section (fb) at muon collider	
	at $\sqrt{s} = 3$ TeV	at $\sqrt{s} = 10$ TeV
γ+MET	5.3×10^{-7}	4.9×10^{-8}
Z+MET	1.1×10^{-5}	1.5×10^{-6}
$b\bar{b}$+MET	2.7×10^{-3}	4.5×10^{-3}
$t\bar{t}$+MET	3.7×10^{-3}	8.9×10^{-3}

DM1000

Final state	Production cross-section (fb) at muon collider	
	at $\sqrt{s} = 3$ TeV	at $\sqrt{s} = 10$ TeV
γ+MET	3.5×10^{-9}	1.3×10^{-10}
Z+MET	4.4×10^{-8}	2.2×10^{-6}
$b\bar{b}$+MET	3.7×10^{-8}	2.0×10^{-5}
$t\bar{t}$+MET	7.8×10^{-9}	3.7×10^{-5}

Collider Phenomenology, Challenging Scenarios

$\mu^+ \rightarrow \leftarrow \mu^-$

DM400

Final state	Production cross-section (fb) at muon collider	
	at $\sqrt{s} = 3$ TeV	at $\sqrt{s} = 10$ TeV
γ+MET	5.3×10^{-7}	4.9×10^{-8}
Z+MET	1.1×10^{-5}	1.5×10^{-6}
$b\bar{b}$+MET	2.7×10^{-3}	4.5×10^{-3}
$t\bar{t}$+MET	3.7×10^{-3}	8.9×10^{-3}

DM1000

Final state	Production cross-section (fb) at muon collider	
	at $\sqrt{s} = 3$ TeV	at $\sqrt{s} = 10$ TeV
γ+MET	3.5×10^{-9}	1.3×10^{-10}
Z+MET	4.4×10^{-8}	2.2×10^{-6}
$b\bar{b}$+MET	3.7×10^{-8}	2.0×10^{-5}
$t\bar{t}$+MET	7.8×10^{-9}	3.7×10^{-5}

LHC

Process	Production cross-section (fb) at $\sqrt{s} = 14$ TeV	
	DM400	**DM1000**
GGF	0.016	1.27×10^{-4}
VBF	0.001	4.7×10^{-6}
BBH	0.008	1.96×10^{-6}

FCC-hh

Process	Production cross-section (fb) at $\sqrt{s} = 100$ TeV	
	DM400	**DM1000**
GGF	1.456	0.117
VBF	0.039	1.182
BBH	0.264	0.029

arXiv: 2504.14529

$$V_{SM} = -\mu^2\Phi^\dagger\Phi + \lambda(\Phi^\dagger\Phi)^2$$

?

- Dark Matter (DM)
- 95 GeV Excess

$$V_{2HDMS} = V_{2HDM} + V_S$$

- Type II
- U(1), Z_2, Z_2'
- DM candidate A_s

Constraints:
- Theoretical: bfb, unitarity
- Experimental: HiggsBounds, Planck, LUX-ZEPLIN, Fermi-LAT

*including 95 GeV excess

Dark Matter (DM) Phenomenology

(Relic Density, Indirect Detection, Direct Detection)

SARAH
SPheno
micrOMEGAs

Collider Phenomenology

(HL-LHC, Future Lepton Colliders)

Pythia
Delphes
MadAnalysis
WHIZARD
Madgraph

Collider Phenomenology, Main Results

HiLumi HL-LHC PROJECT

Process	Benchmark	Significance
GGF	**DM55$_{w95}$**	0.30σ
GGF	**DM70**	0.55σ
VBF	**DM70**	1.94σ
BBH	**DM156$_{w95}$**	1.95σ

$e^+ \rightarrow \leftarrow e^-$

Final State	Benchmark	$\sqrt{s}$	Significance
Z+MET	**DM55$_{w95}$**	250 GeV	11σ ($1\,ab^{-1}$)
Z+MET	**DM70**	250 GeV	3σ ($3\,ab^{-1}$)
Z+MET	**DM55$_{w95}$**	500 GeV	3.6σ ($1\,ab^{-1}$)
Z+MET	**DM70**	500 GeV	1.5σ ($3\,ab^{-1}$)
Z+MET	**DM55$_{w95}$**	1 TeV	2.4σ ($3\,ab^{-1}$)
Z+MET	**DM70**	1 TeV	0.36σ ($3\,ab^{-1}$)

$\mu^+ \rightarrow \leftarrow \mu^-$

Final State	Benchmark	$\sqrt{s}$	Significance
$b\bar{b}$+MET	**DM156$_{w95}$**	3 TeV	6.3σ ($3\,ab^{-1}$)
γ+MET	**DM156$_{w95}$**	1 TeV	3σ ($3ab^{-1}$), 5.3σ ($10ab^{-1}$)
$t\bar{t}$+MET	**DM1000$_{w95}$**	10 TeV	2.9σ ($10\,ab^{-1}$)

[Credit: Kateryna Radchenko]

arXiv: 2504.14529

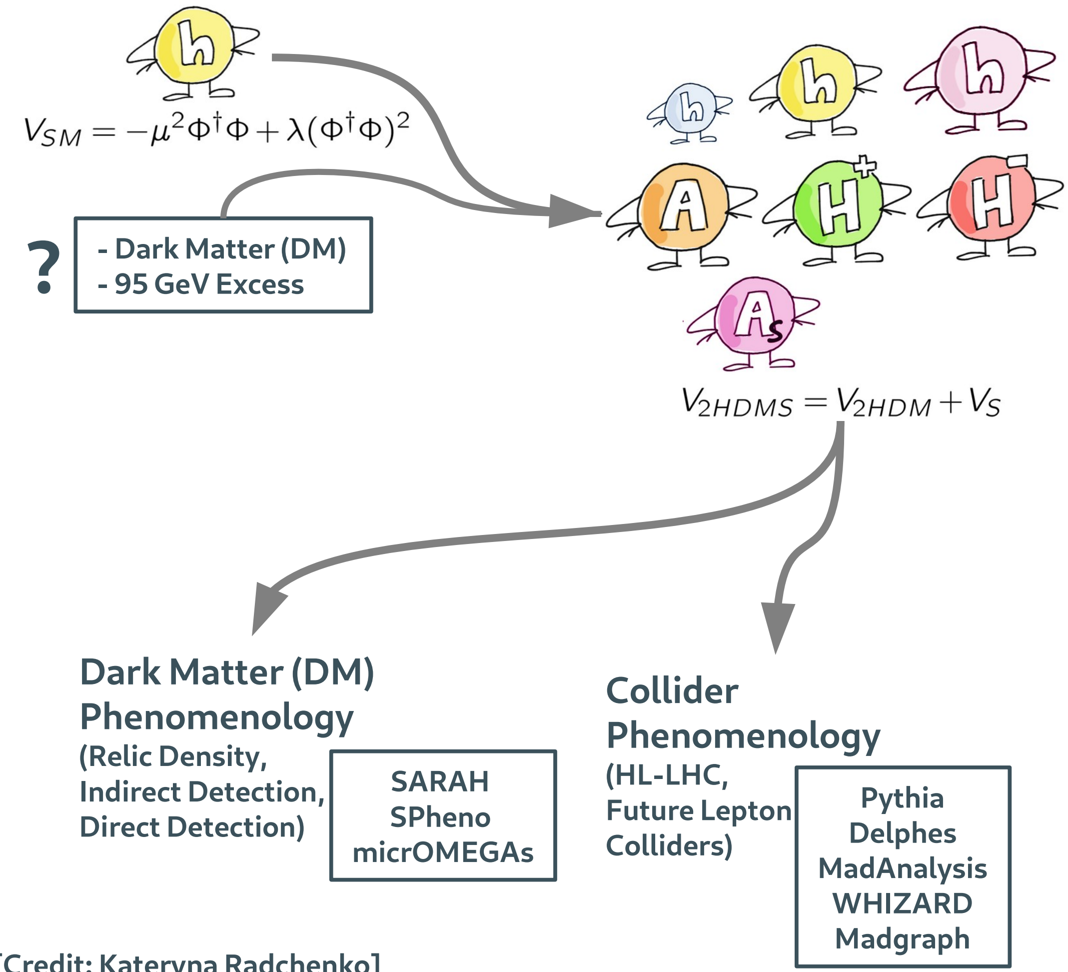

[Credit: Kateryna Radchenko]

Conclusion

- DM search at future colliders:
  - 6 BPs (light, intermediate, heavy)
  - satisfying all DM constraints
- Best prospects for **intermediate and heavy BPs at $\mu^+\mu^-$ colliders**
  - potential improvement with beam polarization
- Best prospects for **light BPs at e^+e^- colliders**
- Challenging scenarios could be probed at FCC-hh

arXiv: 2504.14529

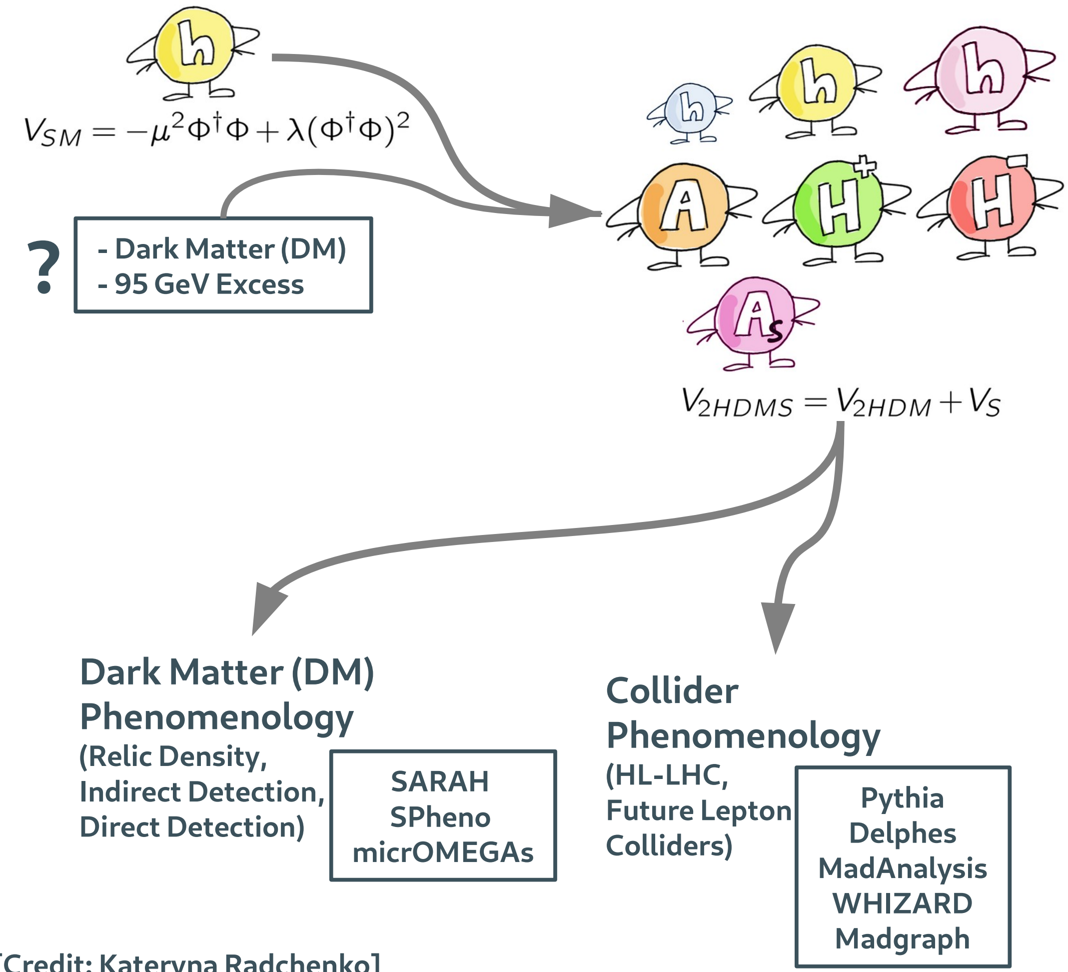

[Credit: Kateryna Radchenko]

Conclusion

- DM search at future colliders:
  - 6 BPs (light, intermediate, heavy)
  - satisfying all DM constraints
- Best prospects for **intermediate and heavy BPs at $\mu^+\mu^-$ colliders**
  - potential improvement with beam polarization
- Best prospects for **light BPs at e^+e^- colliders**
- Challenging scenarios could be probed at FCC-hh

Thank you!

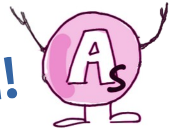

Backup

Backup

m_{h_1}	m_{h_2}	m_{h_3}	m_A	$m_{H^\pm}$	χ^2
95.4 GeV	125.09 GeV	650 GeV	800 GeV	800 GeV	1.26
m_{A_S}	$\lambda_1' - 2\lambda_4'$	$\lambda_2' - 2\lambda_5'$	$\lambda_1'' - \lambda_3''$	$\tan\beta$	
55.596 GeV	0.0020912	0.00074611	−0.025735	2	
v_S	$\tilde{\mu}$	α_1	α_2	α_3	
300 GeV	650 GeV	−1.932	1.272	1.484	

Table 23: The benchmark point $\mathbf{DM55_{w95}}$ in the mass basis.

m_{h_1}	m_{h_2}	m_{h_3}	m_A	$m_{H^\pm}$	χ^2
95.4 GeV	125.09 GeV	700 GeV	700 GeV	700 GeV	0.422
m_{A_S}	$\lambda_1' - 2\lambda_4'$	$\lambda_2' - 2\lambda_5'$	$\lambda_1'' - \lambda_3''$	$\tan\beta$	
156 GeV	12.753	−0.31351	−2.6747	6.6	
v_S	$\tilde{\mu}$	α_1	α_2	α_3	
239.86 GeV	700 GeV	1.4661	1.1920	−1.5989	

Table 24: The benchmark point $\mathbf{DM156_{w95}}$ in the mass basis.

m_{h_1}	m_{h_2}	m_{h_3}	m_A	$m_{H^\pm}$	χ^2
95.4 GeV	125.09 GeV	2950 GeV	2950 GeV	2950 GeV	2.13
m_{A_S}	$\lambda_1' - 2\lambda_4'$	$\lambda_2' - 2\lambda_5'$	$\lambda_1'' - \lambda_3''$	$\tan\beta$	
1000 GeV	21.231	0	−1.4153	5	
v_S	$\tilde{\mu}$	α_1	α_2	α_3	
10005 GeV	2949.29 GeV	−1.769	1.250	1.569	

Table 25: The benchmark point $\mathbf{DM1000_{w95}}$ in the mass basis.

m_{h_1}	m_{h_2}	m_{h_3}	m_A	$m_{H^\pm}$
800 GeV	125.09 GeV	150 GeV	800 GeV	800 GeV
m_{A_S}	$\lambda_1' - 2\lambda_4'$	$\lambda_2' - 2\lambda_5'$	$\lambda_1'' - \lambda_3''$	$\tan\beta$
70 GeV	−0.10783	0.063127	−0.47818	1.3728
v_S	$\tilde{\mu}$	α_1	α_2	α_3
219.05 GeV	751.54 GeV	−0.60016	0.042445	−0.054807

Table 26: The benchmark point **DM70** in the mass basis.

m_{h_1}	m_{h_2}	m_{h_3}	m_A	$m_{H^\pm}$
800 GeV	125.09 GeV	900 GeV	800 GeV	800 GeV
m_{A_S}	$\lambda_1' - 2\lambda_4'$	$\lambda_2' - 2\lambda_5'$	$\lambda_1'' - \lambda_3''$	$\tan\beta$
400 GeV	0.077784	0.036923	−0.42725	2.1309
v_S	$\tilde{\mu}$	α_1	α_2	α_3
587.17 GeV	755.39 GeV	−0.41245	−0.0086501	−0.0055431

Table 27: The benchmark point **DM400** in the mass basis.

m_{h_1}	m_{h_2}	m_{h_3}	m_A	$m_{H^\pm}$
800 GeV	125.09 GeV	2900 GeV	800 GeV	800 GeV
m_{A_S}	$\lambda_1' - 2\lambda_4'$	$\lambda_2' - 2\lambda_5'$	$\lambda_1'' - \lambda_3''$	$\tan\beta$
1000 GeV	0.32873	0.21320	−0.41541	1.3414
v_S	$\tilde{\mu}$	α_1	α_2	α_3
2271.3 GeV	768.14 GeV	−0.54917	0.036530	−0.056095

Table 28: The benchmark point **DM1000** in the mass basis.

Backup

m_{h_1}	m_{h_2}	m_{h_3}	m_A	$m_{H^\pm}$	χ^2
95.4 GeV	125.09 GeV	650 GeV	800 GeV	800 GeV	1.26
m_{A_S}	$\lambda'_1 - 2\lambda'_4$	$\lambda'_2 - 2\lambda'_5$	$\lambda''_1 - \lambda''_3$	$\tan\beta$	
55.596 GeV	0.0020912	0.00074611	-0.025735	2	
v_S	$\tilde{\mu}$	α_1	α_2	α_3	
300 GeV	650 GeV	-1.932	1.272	1.484	

Table 23: The benchmark point $\mathbf{DM55_{w95}}$ in the mass basis.

m_{h_1}	m_{h_2}	m_{h_3}	m_A	$m_{H^\pm}$	χ^2
95.4 GeV	125.09 GeV	700 GeV	700 GeV	700 GeV	0.422
m_{A_S}	$\lambda'_1 - 2\lambda'_4$	$\lambda'_2 - 2\lambda'_5$	$\lambda''_1 - \lambda''_3$	$\tan\beta$	
156 GeV	12.753	-0.31351	-2.6747	6.6	
v_S	$\tilde{\mu}$	α_1	α_2	α_3	
239.86 GeV	700 GeV	1.4661	1.1920	-1.5989	

Table 24: The benchmark point $\mathbf{DM156_{w95}}$ in the mass basis.

m_{h_1}	m_{h_2}	m_{h_3}	m_A	$m_{H^\pm}$	χ^2
95.4 GeV	125.09 GeV	2950 GeV	2950 GeV	2950 GeV	2.13
m_{A_S}	$\lambda'_1 - 2\lambda'_4$	$\lambda'_2 - 2\lambda'_5$	$\lambda''_1 - \lambda''_3$	$\tan\beta$	
1000 GeV	21.231	0	-1.4153	5	
v_S	$\tilde{\mu}$	α_1	α_2	α_3	
10005 GeV	2949.29 GeV	-1.769	1.250	1.569	

Table 25: The benchmark point $\mathbf{DM1000_{w95}}$ in the mass basis.

Benchmarks with a 95 GeV scalar

For the benchmarks, with a scalar at 95 GeV as a part of the mass spectrum, we have ensured that its signal strengths satisfy the following.

The lightest scalar h_1 has a mass of 95.4 GeV and plays the role of a scalar particle responsible for the observed signal strengths, which are for LEP in the $b\bar{b}$ mode ($\sim 2\sigma$) [5] and LHC in the $\gamma\gamma$ mode ($\sim 3\sigma$) [6, 7]:

$$\mu^{b\bar{b}}_{\text{LEP}} = 0.117^{+0.057}_{-0.057}, \qquad \mu^{\gamma\gamma}_{\text{LHC-combined}} = 0.24^{+0.09}_{-0.08}. \tag{4.1}$$

We calculate the combined $\chi^2 = \chi^2_{b\bar{b}} + \chi^2_{\gamma\gamma}$ values according to Ref. [8] and [9] and provide them in the Appendix, Table 23 - 25.

Backup, Collider Pheno, HL-LHC

$$\not{M}^2 = (p_{in} - p_{out})^2$$

$$\sigma^{w_i} = \frac{\sigma^{4f} + w_i \sigma^{5f}}{1 + w_i}$$

$$w_i = ln(\frac{m_{h_i}}{m_b}) - 2$$

Gluon Fusion

We consider the final state mono-jet + MET from the gluon fusion production channel. For the collider analyses, we use the following cuts [70]:

- **C1**: The final state consists of up to four jets with $p_T > 30$ GeV and $|\eta| < 2.8$.
- **C2**: We demand a large $\not{E}_T > 250$ GeV.
- **C3**: The hardest leading jet has $p_T > 250$ GeV with $|\eta| < 2.4$.
- **C4**: We demand $\Delta\Phi(j, \not{E}_T) > 0.4$ for all jets and $\Delta\Phi(j, \not{E}_T) > 0.6$ for the leading jet.
- **C5**: A lepton-veto is imposed for electrons with $p_T > 20$ GeV and $|\eta| < 2.47$ and muons with $p_T > 10$ GeV and $|\eta| < 2.5$.

The SM background of 7.07 pb is obtained from the mono-jet + $\not{E}_T$ search studied in Ref. [71].

Vector Boson Fusion

We consider the final state two forward-jets + MET from the vector boson fusion production channel. For the collider analyses, we use the following cuts [72]:

- **D1**: The final state consists of at least two jets with $p_T(j_1) > 80$ and $p_T(j_2) > 40$ GeV and $\Delta\Phi(j_i, \not{E}_T) > 0.5$.
- **D2**: We demand $\eta(j_1 j_2) < 0$ and $\Delta\Phi j_1 j_2 < 1.5$.
- **D3**: We demand $|\Delta\eta|_{jj} > 3.0$.
- **D4**: The invariant mass of the two forward jets is required to be large, i.e, $M_{jj} > 600$ GeV.
- **D5**: We demand $\not{E}_T > 200$ GeV.
- **D6**: Furthermore, a lepton veto is imposed for electrons with $p_T > 20$ GeV or muons with $p_T > 10$ GeV.

$b\bar{b}$ Higgs associated production

- **E1**: The final state consists of two b jets and no photons or leptons. We demand $\Delta R(b_1, b_2) > 0.4$, $p_T(b_1) > 150$ GeV and $p_T(b_2) > 100$ GeV.
- **E2**: We demand a large missing transverse momenta (MET) $\not{E}_T > 200$ GeV to reduce SM background.
- **E3**: We demand the invariant mass of the $b\bar{b}$ pair (as seen in Fig. 5) is outside the Z (76 GeV $< M(b\bar{b}) <$ 105 GeV) or SM Higgs mass window (115 GeV $< M(b\bar{b}) <$ 135 GeV) to remove background contributions from on-shell Z or Higgs bosons.
- **E4**: Further, we demand $M(b\bar{b}) > 200$ GeV to reduce SM background contributions.

Backup, Collider Phenomenology, HL-LHC

Process	Production cross-section (fb) at $\sqrt{s} = 14$ TeV		
	DM55$_{\mathbf{w95}}$	**DM156$_{\mathbf{w95}}$**	**DM70**
GGF($h_2 \to A_S A_S$)	533.9	-	19.29×10^3
GGF($h_3 \to A_S A_S$)	-	0.015	-
VBF($h_2 \to A_S A_S$)	54.33	-	2.72×10^3
VBF($h_3 \to A_S A_S$)	-	0.134	0.0022
BBH (($b\bar{b}h_2 \to A_S A_S$))	21.6	-	0.137
BBH (($b\bar{b}h_3 \to A_S A_S$))	-	47.24	-

Table 4: The production cross-sections at leading order (LO) of the relevant processes at $\sqrt{s} = 14$ TeV at LHC. All cross-sections below 10^{-6} fb are denoted by '-'. For $b\bar{b}h_i$, with $i = 2, 3$, we use the Santander matched cross-section as defined in the text.

Process	Production cross-section (fb) at $\sqrt{s} = 100$ TeV		
	DM55$_{\mathbf{w95}}$	**DM156$_{\mathbf{w95}}$**	**DM70**
GGF($h_2 \to A_S A_S$)	10.1×10^5	-	4.09×10^5
GGF($h_3 \to A_S A_S$)	-	1.596	-
VBF($h_2 \to A_S A_S$)	5.97×10^2	-	81.87
VBF($h_3 \to A_S A_S$)	-	3.12	-
BBH($h_2 \to A_S A_S$)	6.43×10^2	-	17.2×10^3
BBH($h_3 \to A_S A_S$)	-	5.00	-

Table 10: The production cross-sections at leading order (LO) of the relevant processes for the benchmarks **DM55$_{\mathbf{w95}}$**, **DM156$_{\mathbf{w95}}$** and **DM70** at $\sqrt{s} = 100$ TeV. For BBH we use the Santander matched cross-section as defined in the text.

Process	Production cross-section (fb) at $\sqrt{s} = 14$ TeV		
	DM400	**DM1000**	**DM1000$_{\mathbf{w95}}$**
GGF($h_3 \to A_S A_S$)	0.013	6.35×10^{-7}	4.5×10^{-6}
VBF($h_3 \to A_S A_S$)	0.0008	-	-
BBH($h_3 \to A_S A_S$)	0.007	-	-

Table 5: The production cross-sections at leading order (LO) of the relevant processes for the benchmarks **DM400**, **DM1000** and **DM1000$_{\mathbf{w95}}$** at $\sqrt{s} = 14$ TeV at LHC. For $b\bar{b}h_3$ we use the Santander matched cross-section as defined in the text.

Benchmark	Cross-section after cuts (fb)
DM156$_{\mathbf{w95}}$	0.357
SM Background	
$b\bar{b}Z$	18.3
$b\bar{b}\nu\bar{\nu}$	13.46
$t\bar{t}$	66.46
$Z+j$	2.04
hZ	0.012
Total Background	100.27

Table 8: The cross-sections for the signal and backgrounds after applying the cuts **E1-E4** as discussed in the text for signal-background distinction for BBH for HL-LHC at an integrated luminosity of 3000 fb^{-1}.

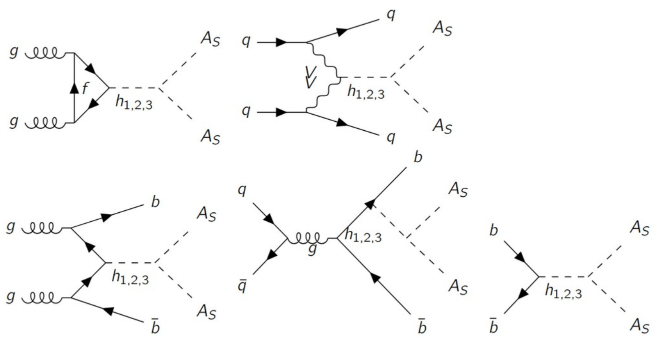

Benchmark	Significance
DM55$_{\mathbf{w95}}$	0.30σ
DM70	0.55σ

Table 6: The signal significance for the signal benchmarks from GGF for HL-LHC at an integrated luminosity of 3000 fb^{-1}.

Benchmark	Significance
DM70	1.94σ

Table 7: The signal significance for the signal benchmarks from VBF for HL-LHC at an integrated luminosity of 3000 fb^{-1}.

Benchmark	Significance
DM156$_{\mathbf{w95}}$	1.95σ

Table 9: The signal significance for the signal from BBH for HL-LHC at an integrated luminosity of 3000 fb^{-1}.

Backup, Collider Phenomenology, e^+e^- Colliders

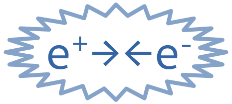

Benchmark	Production cross-section (fb)		
	at $\sqrt{s} = 250$ GeV	at $\sqrt{s} = 500$ GeV	at $\sqrt{s} = 1$ TeV
$\mathbf{DM55_{w95}}$	4.42	1.1	0.24
DM70	0.33	0.15	0.035
$\nu\bar{\nu}Z$ background	503	491	950

Table 11: The Production cross-section for signal (for $\mathbf{DM55_{w95}}$ and **DM70**) and background ($\nu\bar{\nu}Z$) for Z+MET final state at $\sqrt{s}$ = 250 GeV, 500 GeV and 1 TeV e^+e^- collider.

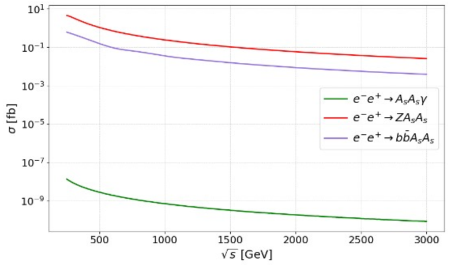

(a) $\mathbf{DM55_{w95}}$

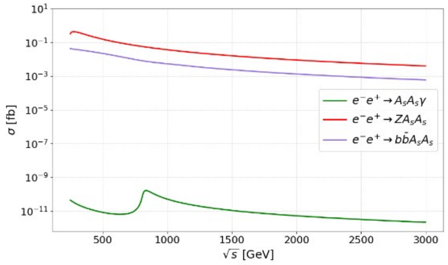

(b) **DM70**

Benchmark	$\sqrt{s}$	Cut	Significance
$\mathbf{DM55_{w95}}$	250 GeV	$\not{M} > 100$ GeV	$11\sigma\ (1ab^{-1})$
DM70	250 GeV	$\not{M} > 130$ GeV	$3\sigma\ (3ab^{-1})$
$\mathbf{DM55_{w95}}$	500 GeV	$\not{M} > 100$ GeV and $\not{M} < 150$ GeV	$3.6\sigma\ (1ab^{-1})$
DM70	500 GeV	$\not{M} > 140$ GeV and $\not{M} < 190$ GeV	$1.5\sigma\ (3ab^{-1})$
$\mathbf{DM55_{w95}}$	1 TeV	$\not{M} > 120$ GeV and $\not{M} < 250$ GeV	$2.4\sigma\ (3ab^{-1})$
DM70	1 TeV	$\not{M} > 120$ GeV and $\not{M} < 250$ GeV	$0.36\sigma\ (3ab^{-1})$

Table 12: The Signal significance (for $\mathbf{DM55_{w95}}$ and **DM70**) for Z+MET final state at $\sqrt{s}$=250 GeV, $\sqrt{s}$=500 GeV and $\sqrt{s}$=1 TeV e^+e^- collider.

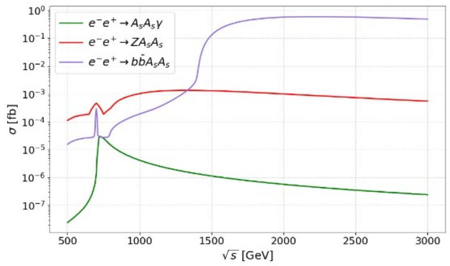

(c) $\mathbf{DM156_{w95}}$

Backup, Collider Phenomenology, e^+e^- Colliders

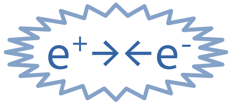

Benchmark	Production cross-section (fb)		
	at $\sqrt{s} = 250$ GeV	at $\sqrt{s} = 500$ GeV	at $\sqrt{s} = 1$ TeV
$\mathbf{DM55_{w95}}$	4.42	1.1	0.24
DM70	0.33	0.15	0.035
$\nu\bar{\nu}Z$ background	503	491	950

Table 11: The Production cross-section for signal (for $\mathbf{DM55_{w95}}$ and **DM70**) and background ($\nu\bar{\nu}Z$) for Z+MET final state at $\sqrt{s}$ = 250 GeV, 500 GeV and 1 TeV e^+e^- collider.

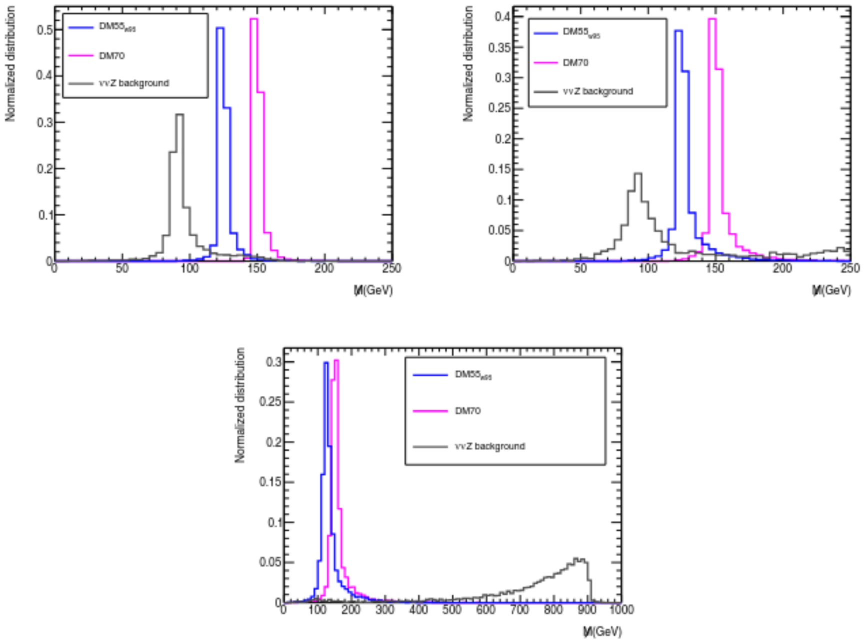

Figure 7: Distribution of missing mass $\not{M}$ for signal (for $\mathbf{DM55_{w95}}$ and **DM70**) and background ($\nu\bar{\nu}Z$) for Z+MET final state at $\sqrt{s}$=250 GeV (top left), $\sqrt{s}$=500 GeV (top right) and $\sqrt{s}$=1 TeV (bottom) e^+e^- collider.

Backup, Collider Phenomenology, $\mu^+\mu^-$ Colliders

$\mu^+ \rightarrow \leftarrow \mu^-$

Benchmark	Production cross-section (fb)	
	at $\sqrt{s} = 3$ TeV	at $\sqrt{s} = 10$ TeV
DM156$_{\mathbf{w95}}$	0.48	0.063
$b\bar{b}\nu\nu$ background	758	1.3
$t\bar{t}$ background	20	1.7

Table 13: The Production cross-section for signal (for **DM156$_{\mathbf{w95}}$**) and background ($b\bar{b}\nu\nu$ and $t\bar{t}$) for $b\bar{b}$+MET final state at $\sqrt{s} = 3$ TeV and 10 TeV muon collider.

Benchmark	Cut	Significance
DM156$_{\mathbf{w95}}$	100 GeV $< m_{bb} <$ 500 GeV	6.3σ $(3ab^{-1})$

Table 14: The Signal significance and corresponding cuts (for **DM156$_{\mathbf{w95}}$**) for $b\bar{b}$+MET final state at $\sqrt{s} = 3$ TeV muon collider.

Benchmark	Production cross-section (fb)at $\sqrt{s} = 1$ TeV
DM156$_{\mathbf{w95}}$	0.23
$\nu\nu\gamma$ background	2.45

Table 15: The Production cross-section for signal (for **DM156$_{\mathbf{w95}}$**) and background ($\nu\nu\gamma$) for γ+MET final state at $\sqrt{s} = 1$ TeV muon collider.

Benchmark	Cut	Significance
DM156$_{\mathbf{w95}}$	690 GeV $< \not{M} <$ 710 GeV	3σ $(3ab^{-1})$, 5.3σ $(10ab^{-1})$

Table 16: The Signal significance and corresponding cuts (for **DM156$_{\mathbf{w95}}$**) for γ+MET final state at $\sqrt{s} = 1$ TeV muon collider.

Benchmark	Production cross-section (fb) at $\sqrt{s} = 10$ TeV
DM1000$_{\mathbf{w95}}$	0.027
$t\bar{t}$+MET background	1.66

Table 17: The Production cross-section for signal (**DM1000$_{\mathbf{w95}}$**) and background ($t\bar{t}$+MET) for $t\bar{t}$+MET final state at $\sqrt{s} = 10$ TeV muon collider.

Benchmark	Cut	Significance
DM1000$_{\mathbf{w95}}$	$m_{bb} < 2$ TeV	2.9σ $(10ab^{-1})$

Table 18: The Signal significance and corresponding cuts (for **DM1000$_{\mathbf{w95}}$**) for $t\bar{t}$+MET final state at $\sqrt{s} = 10$ TeV muon collider.

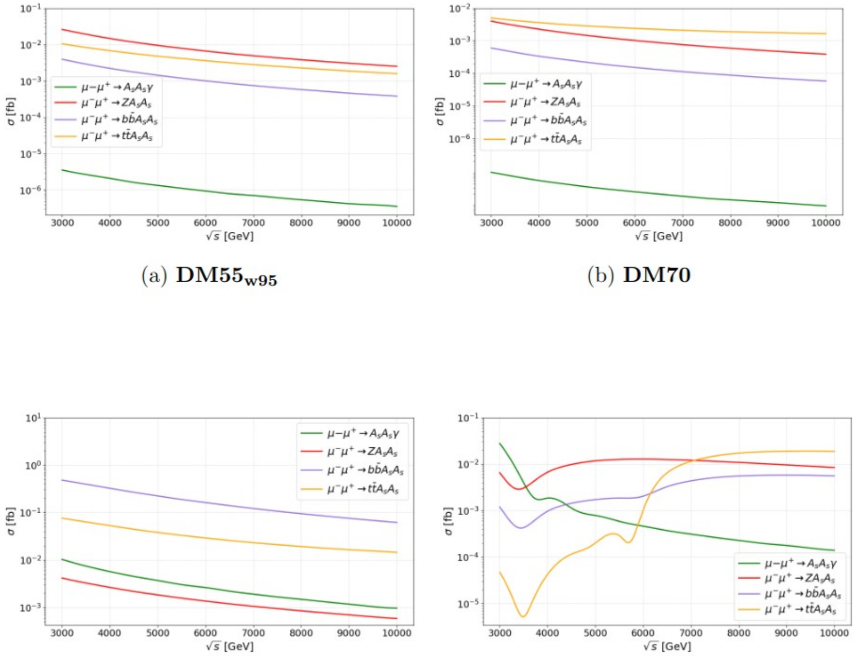

(a) **DM55$_{\mathbf{w95}}$** (b) **DM70**

(c) **DM156$_{\mathbf{w95}}$** (d) **DM1000$_{\mathbf{w95}}$**

Figure 8: Variation of the production cross-section against $\sqrt{s}$ for the final states $A_sA_s\gamma$, ZA_sA_s, $b\bar{b}A_sA_s$, and $t\bar{t}A_sA_s$ at a muon collider, computed using `WHIZARD` [67] for different benchmark points.

Backup

$$0=\frac{\partial V}{\partial \Phi_1}\Big|_{\substack{\Phi_1=\langle\Phi_1\rangle\\ \Phi_2=\langle\Phi_2\rangle\\ S=\langle S\rangle}}=\frac{1}{\sqrt{2}}[m_{11}^2 v_1-m_{12}^2 v_2+\frac{\lambda_1}{2}v_1^3+\frac{\lambda_{345}}{2}v_1 v_2^2+(\frac{\lambda_1'}{2}v_1+\lambda_4' v_1)v_S^2] \tag{A.1a}$$

$$0=\frac{\partial V}{\partial \Phi_2}\Big|_{\substack{\Phi_1=\langle\Phi_1\rangle\\ \Phi_2=\langle\Phi_2\rangle\\ S=\langle S\rangle}}=\frac{1}{\sqrt{2}}[m_{22}^2 v_2-m_{12}^2 v_1+\frac{\lambda_2}{2}v_2^3+\frac{\lambda_{345}}{2}v_1^2 v_2+(\frac{\lambda_2'}{2}v_2+\lambda_5' v_2)v_S^2] \tag{A.1b}$$

$$\begin{aligned}0=\frac{\partial V}{\partial S}\Big|_{\substack{\Phi_1=\langle\Phi_1\rangle\\ \Phi_2=\langle\Phi_2\rangle\\ S=\langle S\rangle}}&=\frac{1}{\sqrt{2}}[m_S^2 v_S+m_S'^2 v_S+\frac{\lambda_1''}{12}v_S^3+\frac{\lambda_2''}{3}v_S^3+\frac{\lambda_3''}{4}v_S^3\\&+\frac{v_S}{2}(\lambda_1' v_1^2+\lambda_2' v_2^2)+v_S(\lambda_4' v_1^2+\lambda_5' v_2^2)].\end{aligned} \tag{A.1c}$$

$$R=\begin{pmatrix} c_{\alpha_1}c_{\alpha_2} & s_{\alpha_1}c_{\alpha_2} & s_{\alpha_2}\\ -s_{\alpha_1}c_{\alpha_3}-c_{\alpha_1}s_{\alpha_2}s_{\alpha_3} & c_{\alpha_1}c_{\alpha_3}-s_{\alpha_1}s_{\alpha_2}s_{\alpha_3} & c_{\alpha_2}s_{\alpha_3}\\ s_{\alpha_1}s_{\alpha_3}-c_{\alpha_1}s_{\alpha_2}c_{\alpha_3} & -c_{\alpha_1}s_{\alpha_3}-s_{\alpha_1}s_{\alpha_2}c_{\alpha_3} & c_{\alpha_2}c_{\alpha_3}\end{pmatrix}$$

$$\begin{aligned}
m_{12}^2&=\tilde{\mu}^2\cdot\sin\beta\cos\beta\\
\lambda_1&=\frac{1}{v^2\cos^2\beta}(\Sigma_{i=1}^3 m_i^2 R_{i1}^2-\tilde{\mu}^2\sin^2\beta),\\
\lambda_2&=\frac{1}{v^2\sin^2\beta}(\Sigma_{i=1}^3 m_i^2 R_{i2}^2-\tilde{\mu}^2\cos^2\beta),\\
\lambda_3&=\frac{1}{v^2}(\frac{1}{\sin\beta\cos\beta}\Sigma_{i=1}^3 m_i^2 R_{i1}R_{i2}-\tilde{\mu}^2+2m_{H^\pm}^2),\\
\lambda_4&=\frac{1}{v^2}(m_A^2+\tilde{\mu}^2-2m_{H^\pm}^2),\\
\lambda_5&=\frac{1}{v^2}(-m_A^2+\tilde{\mu}^2),\\
\lambda_1'&=\frac{1}{2}(\frac{1}{vv_S\cos\beta}\Sigma_{i=1}^3 m_i^2 R_{i1}R_{i3}+\lambda_{14}'),\\
\lambda_2'&=\frac{1}{2}(\frac{1}{vv_S\sin\beta}\Sigma_{i=1}^3 m_i^2 R_{i2}R_{i3}+\lambda_{25}'),\\
\lambda_4'&=\frac{1}{4}(\frac{1}{vv_S\cos\beta}\Sigma_{i=1}^3 m_i^2 R_{i1}R_{i3}-\lambda_{14}'),\\
\lambda_5'&=\frac{1}{4}(\frac{1}{vv_S\sin\beta}\Sigma_{i=1}^3 m_i^2 R_{i2}R_{i3}-\lambda_{25}'),\\
\lambda_1''&=\frac{3}{4v_S^2}(\Sigma_{i=1}^3 m_i^2 R_{i3}^2+\frac{v_S^2}{2}\lambda_{13}''),\\
\lambda_2''&=\lambda_1'',\\
\lambda_3''&=\frac{3}{4v_S^2}(\Sigma_{i=1}^3 m_i^2 R_{i3}^2+\frac{5v_S^2}{6}\lambda_{13}''),\\
m_S'^2&=-(\frac{1}{2}m_{A_S}^2+\frac{1}{4}\Sigma_{i=1}^3 m_i^2(R_{i3}^2+R_{i1}R_{i3}\frac{v\cos\beta}{v_S}+R_{i2}R_{i3}\frac{v\sin\beta}{v_S})\\
&\quad-\frac{v^2}{4}(\lambda_{14}'\cos^2\beta+\lambda_{25}'\sin^2\beta)+\frac{v_S^2}{8}\lambda_{13}'')
\end{aligned}$$

DM156$_{w95}$

$\mu^+ \rightarrow \leftarrow \mu^-$

Collider Phenomenology, $\mu^+\mu^-$ Colliders

bb+MET

Benchmark	Production cross-section (fb)	
	at $\sqrt{s} = 3$ TeV	at $\sqrt{s} = 10$ TeV
DM156$_{w95}$	0.48	0.063
$b\bar{b}\nu\nu$ background	758	1.3
$t\bar{t}$ background	20	1.7

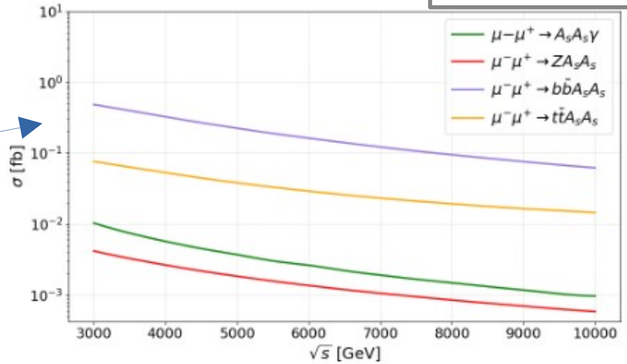

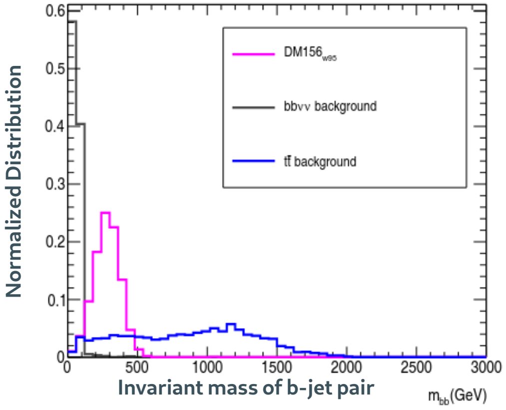

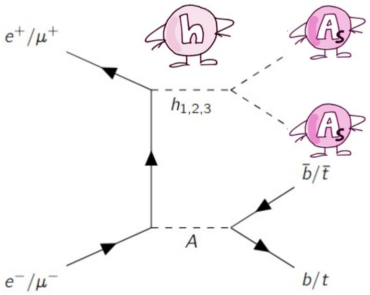

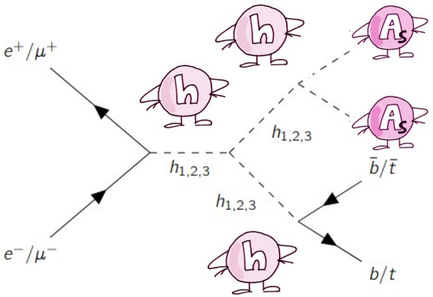

Benchmark	Cut	Significance
DM156$_{w95}$	100 GeV $< m_{bb} <$ 500 GeV	6.3σ $(3ab^{-1})$

μ⁺→←μ⁻

Collider Phenomenology, μ⁺μ⁻ Colliders

bb+MET

Benchmark	Production cross-section (fb)	
	at $\sqrt{s} = 3$ TeV	at $\sqrt{s} = 10$ TeV
DM156$_{w95}$	0.48	0.063
$b\bar{b}\nu\nu$ background	758	1.3
$t\bar{t}$ background	20	1.7

γ+MET

Benchmark	Production cross-section (fb)at $\sqrt{s} = 1$ TeV
DM156$_{w95}$	0.23
$\nu\nu\gamma$ background	2.45

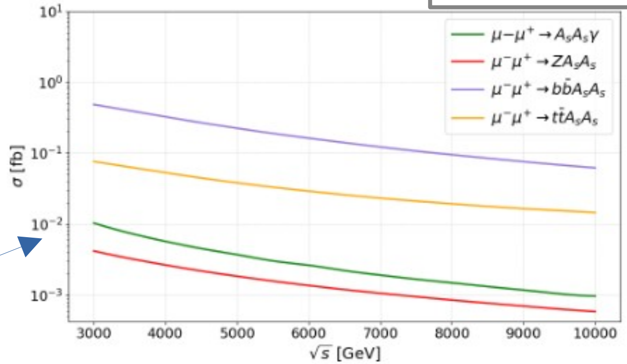

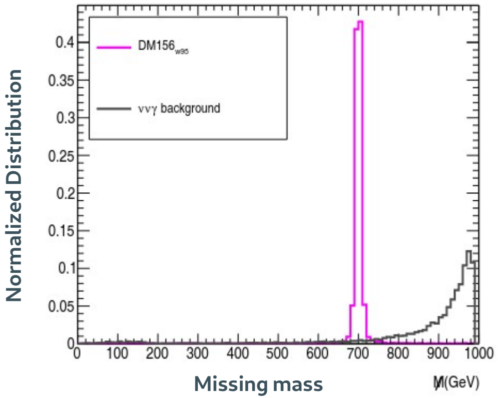

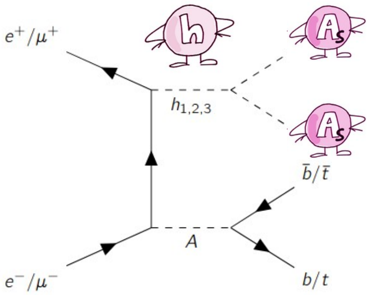

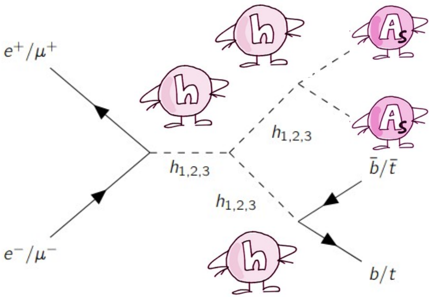

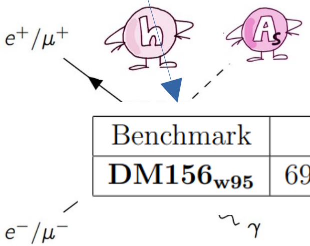

Benchmark	Cut	Significance
DM156$_{w95}$	690 GeV $< \not{M} <$ 710 GeV	3σ $(3ab^{-1})$, 5.3σ $(10ab^{-1})$

DM1000$_{w95}$

μ⁺→←μ⁻

Collider Phenomenology, $\mu^+\mu^-$ Colliders

bb+MET

Benchmark	Production cross-section (fb)	
	at $\sqrt{s} = 3$ TeV	at $\sqrt{s} = 10$ TeV
DM156$_{w95}$	0.48	0.063
$b\bar{b}\nu\nu$ background	758	1.3
$t\bar{t}$ background	20	1.7

γ+MET

Benchmark	Production cross-section (fb)at $\sqrt{s} = 1$ TeV
DM156$_{w95}$	0.23
$\nu\nu\gamma$ background	2.45

tt+MET

Benchmark	Production cross-section (fb) at $\sqrt{s} = 10$ TeV
DM1000$_{w95}$	0.027
$t\bar{t}$+MET background	1.66

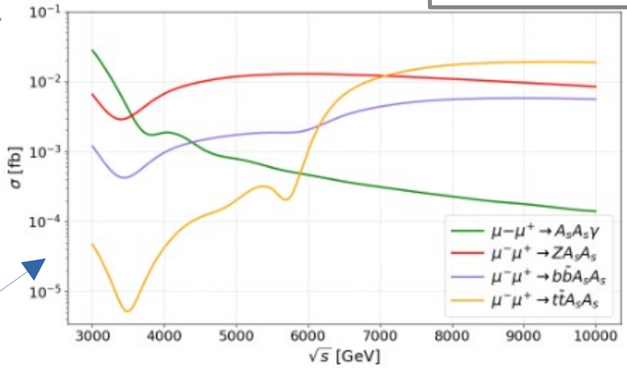

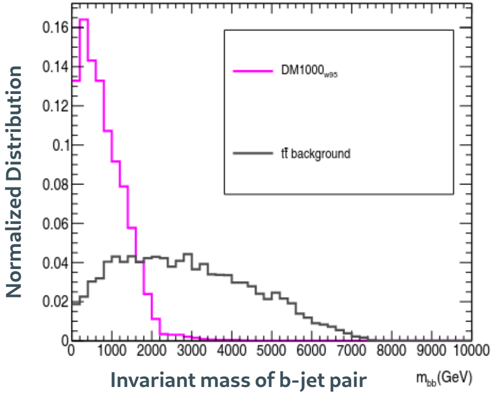

Benchmark	Cut	Significance
DM1000$_{w95}$	$m_{bb} < 2$ TeV	2.9σ $(10ab^{-1})$

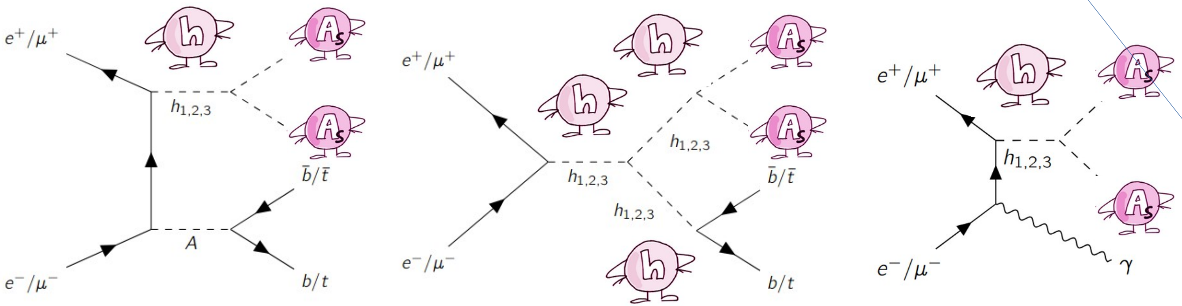

2HDMS Type II, Higgs Sector Potential

[Notation as in: Baum and Shah, arXiv: 1808.02667]

$$\begin{pmatrix} h_1 \\ h_2 \\ h_3 \end{pmatrix} = R(\alpha_{1,2,3}) \begin{pmatrix} \rho_1 \\ \rho_2 \\ \rho_3 \end{pmatrix}$$

$$v = \sqrt{v_1^2 + v_2^2}$$

$$\tan(\beta) = \frac{v_2}{v_1}$$

$$\tilde{\mu}^2 = \frac{m_{12}^2}{\sin\beta\cos\beta}$$

$$\lambda'_{14} = \lambda'_1 - 2\lambda'_4$$

$$\lambda'_{25} = \lambda'_2 - 2\lambda'_5$$

$$\lambda''_{13} = \lambda''_1 - \lambda''_3$$

$$V = V_{2HDM} + V_S$$

$$\begin{aligned} V_{2HDM} = {} & m_{11}^2 \Phi_1^\dagger \Phi_1 + m_{22}^2 \Phi_2^\dagger \Phi_2 - [m_{12}^2 \Phi_1^\dagger \Phi_2 + h.c.] + \frac{\lambda_1}{2} (\Phi_1^\dagger \Phi_1)^2 \\ & + \frac{\lambda_2}{2} (\Phi_2^\dagger \Phi_2)^2 + \lambda_3 (\Phi_1^\dagger \Phi_1)(\Phi_2^\dagger \Phi_2) + \lambda_4 (\Phi_1^\dagger \Phi_2)(\Phi_2^\dagger \Phi_1) \\ & + \left[\frac{\lambda_5}{2} (\Phi_1^\dagger \Phi_2)^2 + h.c. \right] \end{aligned}$$

$$\begin{aligned} V_S = {} & m_S^2 S^\dagger S + \left[\frac{m_S'^2}{2} S^2 + h.c. \right] \\ & + \left[\frac{\lambda''_1}{24} S^4 + h.c. \right] + \left[\frac{\lambda''_2}{6} (S^2 S^\dagger S) + h.c. \right] + \frac{\lambda''_3}{4} (S^\dagger S)^2 \\ & + S^\dagger S [\lambda'_1 \Phi_1^\dagger \Phi_1 + \lambda'_2 \Phi_2^\dagger \Phi_2] + [S^2 (\lambda'_4 \Phi_1^\dagger \Phi_1 + \lambda'_5 \Phi_2^\dagger \Phi_2) + h.c.] \end{aligned}$$

for this study:
$\lambda_2'' = \lambda_1''$

Basis Change:

Interaction Basis Parameters:

$\lambda_1, \lambda_2, \lambda_3, \lambda_4, \lambda_5, m_{12}^2, \tan\beta, v_S, m_S^{2\prime},$
$\lambda'_1, \lambda'_2, \lambda'_4, \lambda'_5, \lambda''_1 = \lambda''_2, \lambda''_3$

$\Downarrow$

Mass Basis Parameters:

$m_{h_1}, m_{h_2}, m_{h_3}, m_A, m_{A_S}, m_{H^\pm}, \alpha_1, \alpha_2, \alpha_3,$
$\tan\beta, v_S, \tilde{\mu}^2, \lambda'_{14}, \lambda'_{25}, \lambda''_{13}$